Electronic Supplementary Material (ESI) for Journal of Materials Chemistry B.

Tunable GUMBOS-Based Sensor Array for Label-Free Detection and Discrimination of Proteins †

Supporting Information

Waduge Indika S. Galpothdeniya[1], Frank R. Fronczek[1], Mingyan Cong[1], Nimisha Bhattarai[1], Noureen Siraj and Isiah M. Warner[1*]

[1]Department of Chemistry, Louisiana State University, Baton Rouge, LA 70803, USA

* Corresponding author: Isiah M. Warner, email: iwarner@lsu.edu, Phone: 1-225-578-2829, Fax: 1-225-578-3458

Materials

Sodium 6-(p-toluidino)-2-naphthalenesulfonate ([Na][TNS]), trihexyl(tetradecyl)phosphonium chloride ([P_{66614}][Cl]), tetrabutylphosphonium bromide ([P_{4444}][Br]), tetraphenylphosphonium chloride ([TPP][Cl]), (4-nitrophenyl)triphenylphosphonium bromide ([4NB][Br]), Benzyltriphenylphosphonium chloride ([BTP][Cl]), anhydrous ethanol (200 proof), anhydrous methylene chloride (DCM), and all proteins were purchased from Sigma-Aldrich, and used as received. Triply deionized water (18.2 MΩ cm) from an Elga model PURELAB ultra water-filtration system was used for preparation of the sodium phosphate buffer (pH 7.4/10 mM).

Synthesis and Characterization of Functional GUMBOS

Briefly, a phosphonium salt (PR_4)[X]; R- hydrocarbon substituent, X- halide) was dissolved in DCM and added onto solid [Na][TNS] at a molar ratio of 1:1.1. Afterwards, a few drops of triply deionized water were added to the reaction mixture in order to collect the resulting byproduct (NaX), and then stirred for 24 h. Afterwards, the DCM layer was separated from the water layer and filtered in order to remove excess [Na][TNS]. Next, the filtrate was washed repeatedly with water in order to remove NaX byproduct. The product was recrystallized using a DCM/water solvent mixture. The final product [PR_4][TNS] was dried by removal of solvents *in vacuo*. Finally, the resultant GUMBOS were characterized by use of electron spray ionization mass spectroscopy (ESI-MS) (Fig. S1 in the supporting information (SI)), and single-crystal X-ray crystallography. The ionic compounds [TPP][TNS], [P_{4444}][TNS], and [BTP][TNS] were found to be crystalline. Crystal data and details of the structural refinement for [TPP][TNS], [P_{4444}][TNS], and [BTP][TNS] are provided in the Table S1 in the SI.

Single-Crystal X-ray Crystallographic Studies

Diffraction data were collected at low temperature on a Bruker Kappa Apex-II DUO diffractometer with Cu Kα (λ = 1.54184 Å) or MoKα radiation (λ = 0.71073 Å). Refinement was by full-matrix

least squares using SHELXL[1,2], with H atoms in idealized positions except for those on N, for which coordinates were refined. [BTP][TNS] was the DCM solvate, and disordered water solvent in [TPP][TNS] was removed using SQUEEZE.[1,2] Crystal data: $[P_{4444}][TNS]$, $[C_{16}H_{36}P][C_{17}H_{14}NO_3S]$, monoclinic $P2_1/c$, a=10.3977(4), b=18.2132(7), c=17.4211(6) Å, β=102.071(3)°, Z=4, T=90K, θ_{max}=59.0° (Cu), R=0.070 for 2612 data with I>2σ(I) (of 4636 unique), 359 parameters, CCDC 1058986; [BTP][TNS], $[C_{25}H_{22}P][C_{17}H_{14}NO_3S]$. CH_2Cl_2, triclinic P1, a=10.0089(4), b=10.4658(4), c=10.8995(4) Å, α=61.537(2), β=78.686(2), γ=66.103(2)°, Z=1, T=90K, θ_{max}=35.0° (Mo), R=0.041 for 11156 data with I>2σ(I) (of 12497 unique), 465 parameters, CCDC 1058985; [TPP][TNS], $[C_{24}H_{20}P][C_{17}H_{14}NO_3S]$. $0.7H_2O$, monoclinic $P2_1/c$, a=14.3436(10), b=13.8575(9), c=18.0804(12) Å, β=112.786(2)°, Z=4, T=90K, θ_{max}=68.8° (Cu), R=0.049 for 5188 data with I>2σ(I) (of 5810 unique), 428 parameters, CCDC 1058984.

Absorption and Fluorescence Studies

A Shimadzu UV-3101PC spectrophotometer was used to acquire absorbance spectra. A Spex Fluorolog-3 spectrofluorimeter (model FL3- 22TAU3; Jobin Yvon, Edison, NJ) was used to perform fluorescence studies. A 1.0 cm path length quartz cuvette (Starna Cells) was used in both absorbance and fluorescence data acquisition. Absorption spectra were collected against an identical cell filled with pH 7.4 phosphate buffer as the blank. Fluorescence studies were performed by adapting a synchronous scan protocol with right angle geometry.[3] A 5.0 mL buffer solution mixed with 50 µL of 0.5 mM ethanolic, TNS-based sensor solution was used as blank in fluorescence studies.

Absolute Quantum Yield Measurements

Absolute quantum yield measurements for all TNS-based GUMBOS were measured using an integrated sphere. A 1.0 cm path length quartz cuvette (Starna Cells) was used for data

acquisition. The TNS-based GUMBOS were prepared at concentrations equivalent to 10 μM in ethanol to obtain quantum yield (φ_{fl}) in ethanol. In order to obtain φ_{fl} in water, 100 μL of 0.5 mM ethanolic TNS-based sensor solution was rapidly introduced into a 5 mL pH 7.4 buffer solution and ultra-sonicated for 5 min prior to measurements.

Octanol-Water Partition Coefficient ($K_{o/w}$)

The $K_{o/w}$ values were determined by use of absorbance measurements obtained from a Shimadzu UV-3101PC spectrophotometer. All absorbance measurements were performed using a 1.0 cm path length quartz cuvette (Starna Cells). Briefly, an equal amount of octanol and water were mixed and left standing overnight until the solubility of the water in octanol is equilibrated. The two phases were then separated into two different containers. Each compound was dissolved in 10 mL of the water saturated octanol to prepare a 1.0 mM stock solution. The 1.0 mM stock solution was then used to prepare 4 dilutions that were used to form a calibration curve based on the absorbance readings and a best-fit line was plotted. One concentration from the calibration curve was then chosen and mixed with an equal volume of the water mentioned in the separation step above. This solution was then allowed to stir for 24 hours. Following the 24 hours, the octanol layer was then extracted and the absorbance was measured. The equation for the line of best-fit from the calibration curves was then used to determine the concentration of compounds within the octanol and water layers for all compounds. The equation $K_{(o/w)} = [octanol\ layer]/[water\ layer]$ was then used to calculate the octanol water partition coefficient.

Development of Predictive Models

In this study, predictive models were developed in order to accurately identify analytes used in each experiment. Fluorescence sensor-response patterns generated by use of the four TNS-based sensors (four TNS-GUMBOS × number of analytes × five replicates) were employed to develop statistical models in each experiment. First, the dimensionality of the predictor space was

reduced using PCA. In most experiments, the first two principal components in PCA accounted for more than 99% variance (except when the input data were normalized). Therefore, only the values of these two components were used to develop predictive models using LDA. Second, the predictive accuracy of each statistical model was assessed separately using cross-validation.

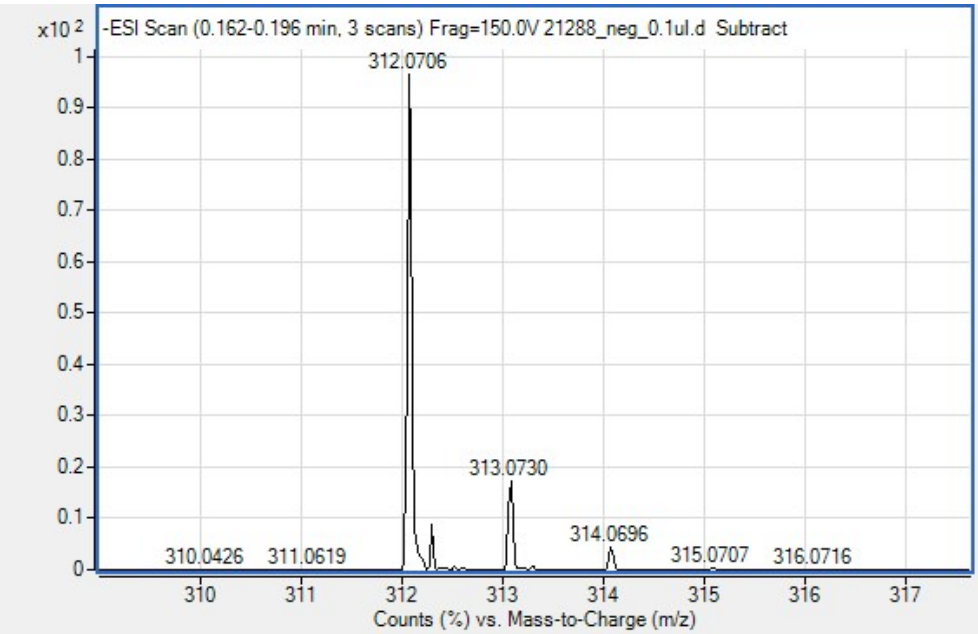

Figure S1-1A Electrospray ionization mass spectrum in negative ion mode for TNS

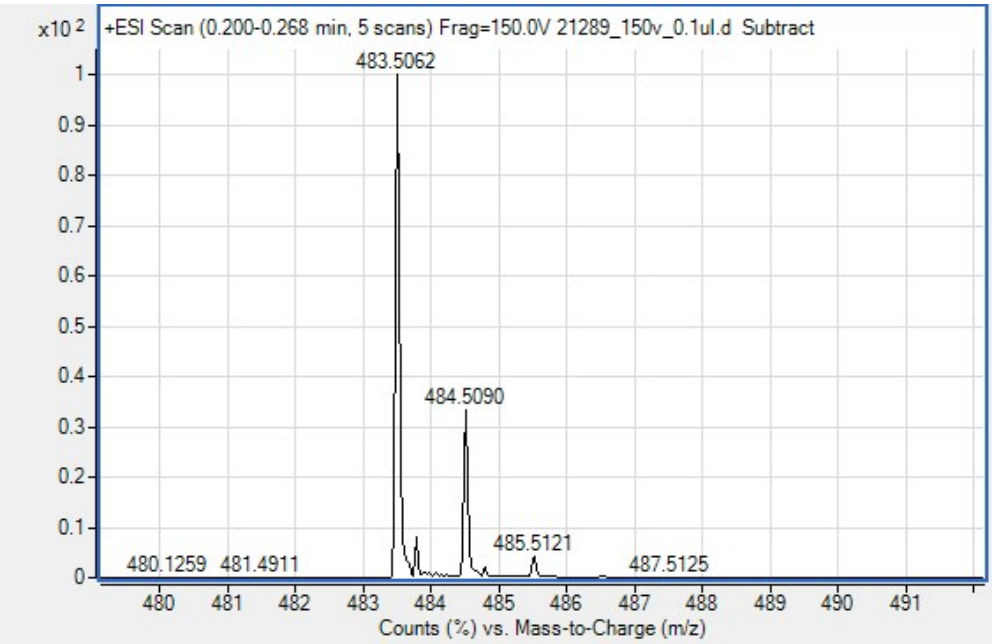

Figure S1-2A Electrospray ionization mass spectrum in positive ion mode for $[P_{66614}][TNS]$

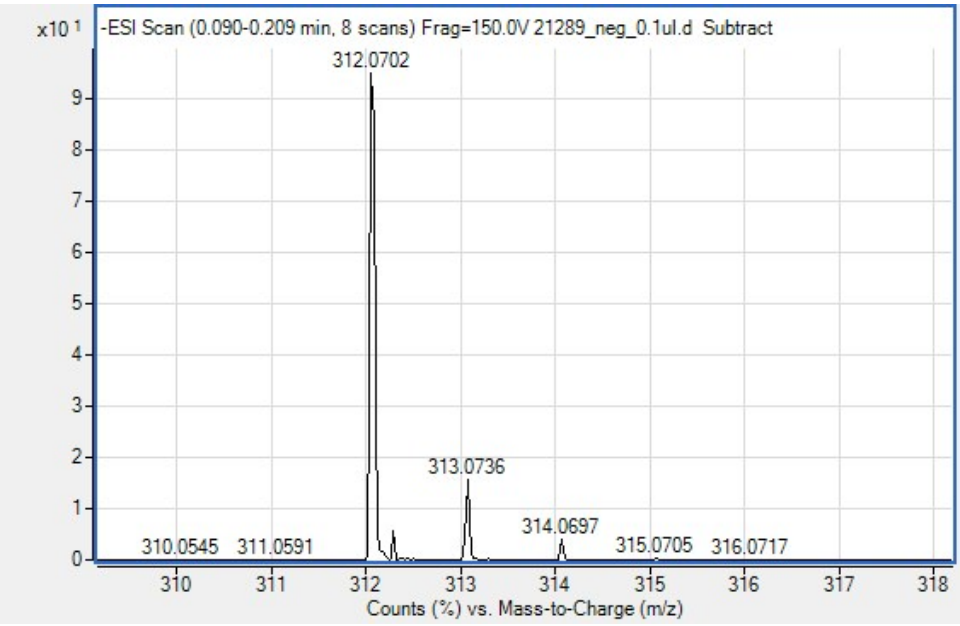

Figure S1-2B Electrospray ionization mass spectrum in negative ion mode for $[P_{66614}][TNS]$

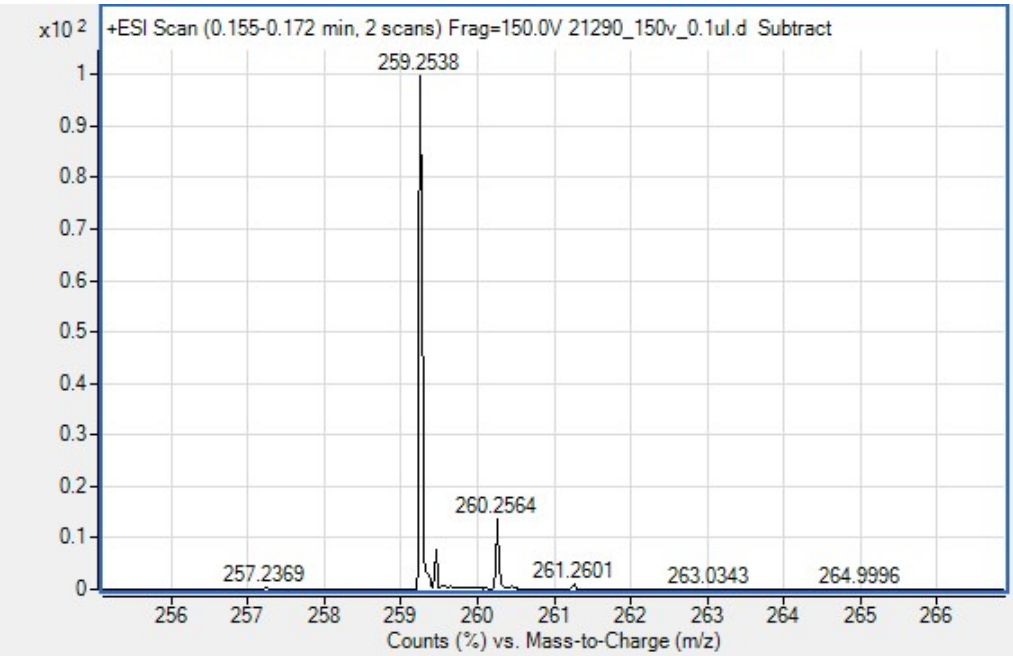

Figure S1-3A Electrospray ionization mass spectrum in positive ion mode for $[P_{4444}][TNS]$

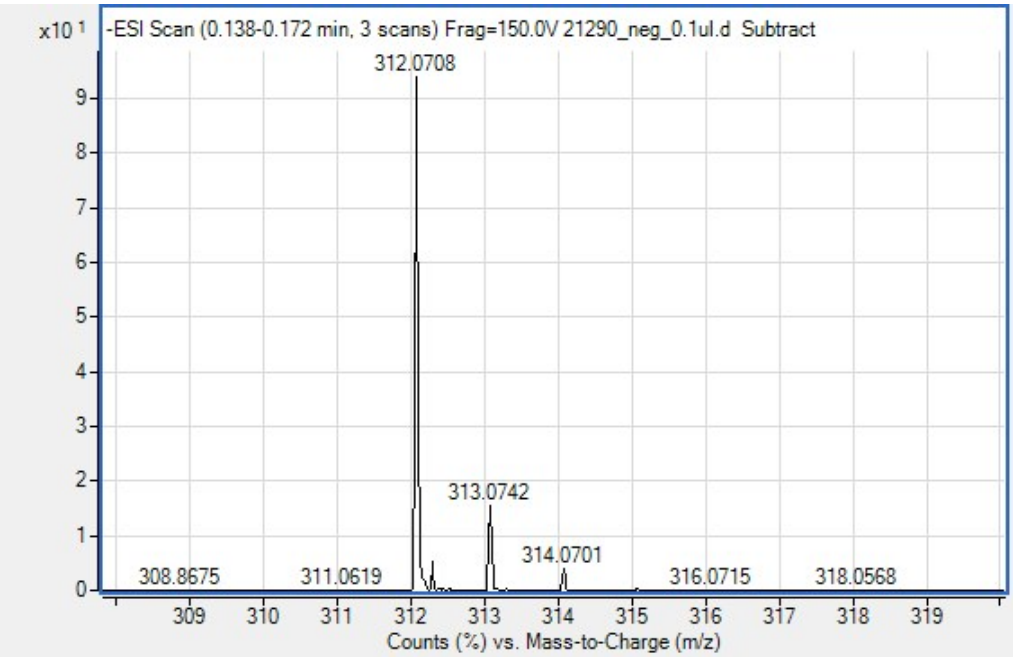

Figure S1-3B Electrospray ionization mass spectrum in negative ion mode for $[P_{4444}][TNS]$

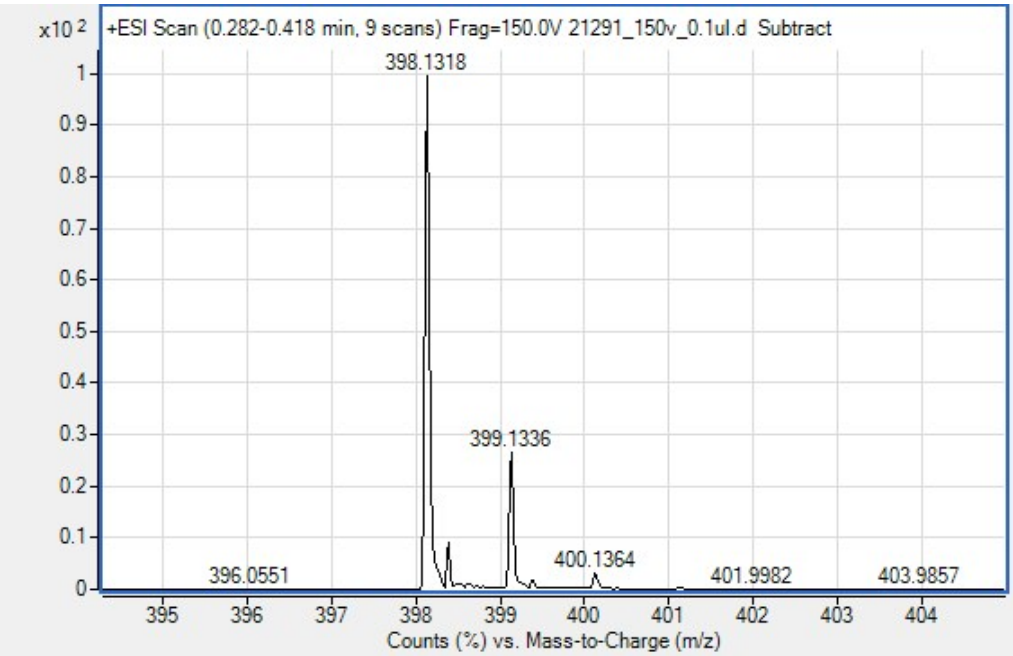

Figure S1-4A Electrospray ionization mass spectrum in positive ion mode for [4NB][TNS]

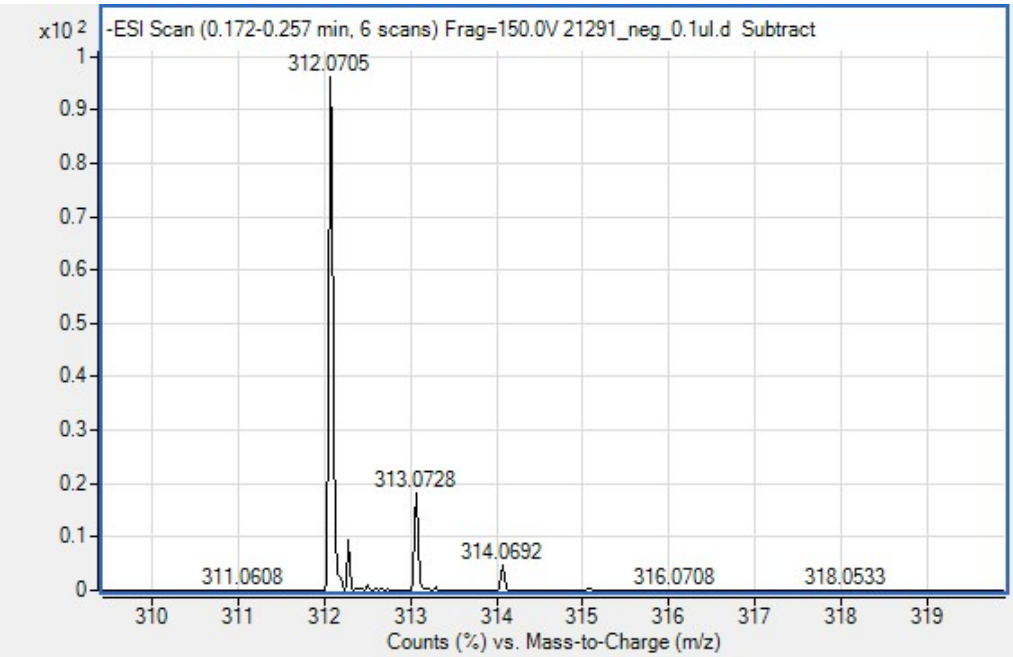

Figure S1-4B Electrospray ionization mass spectrum in negative ion mode for [4NB][TNS]

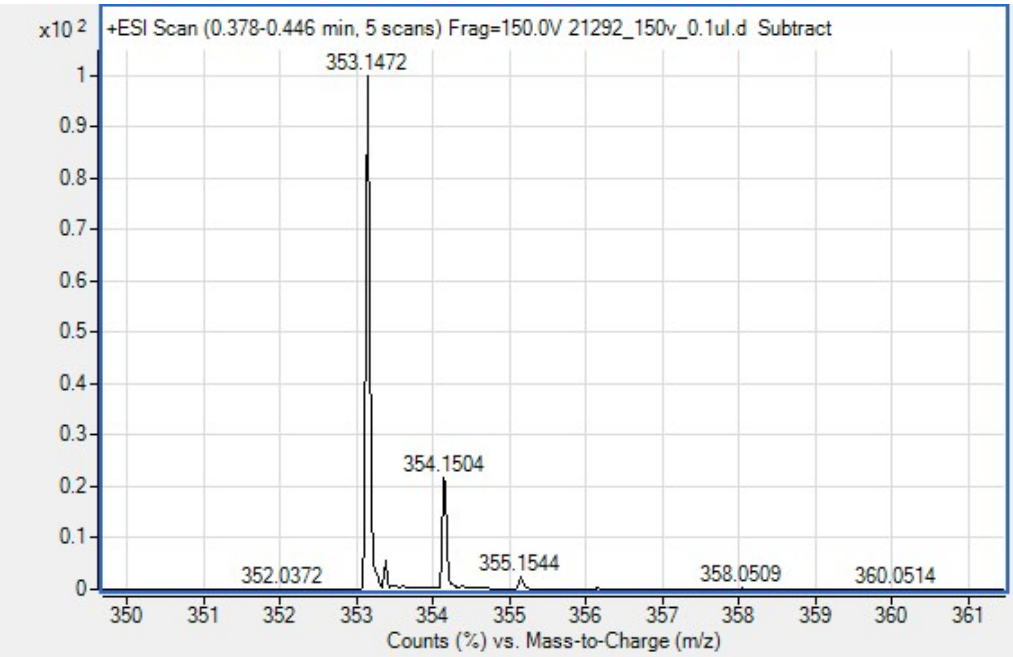

Figure S1-5A Electrospray ionization mass spectrum in positive ion mode for [BTP][TNS]

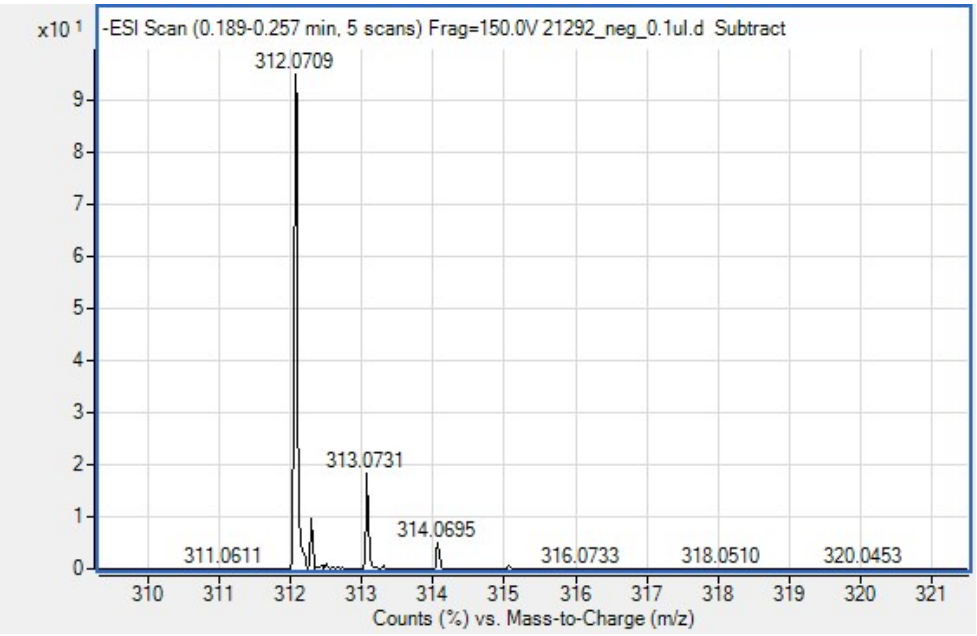

Figure S1-5B Electrospray ionization mass spectrum in negative ion mode for [BTP][TNS]

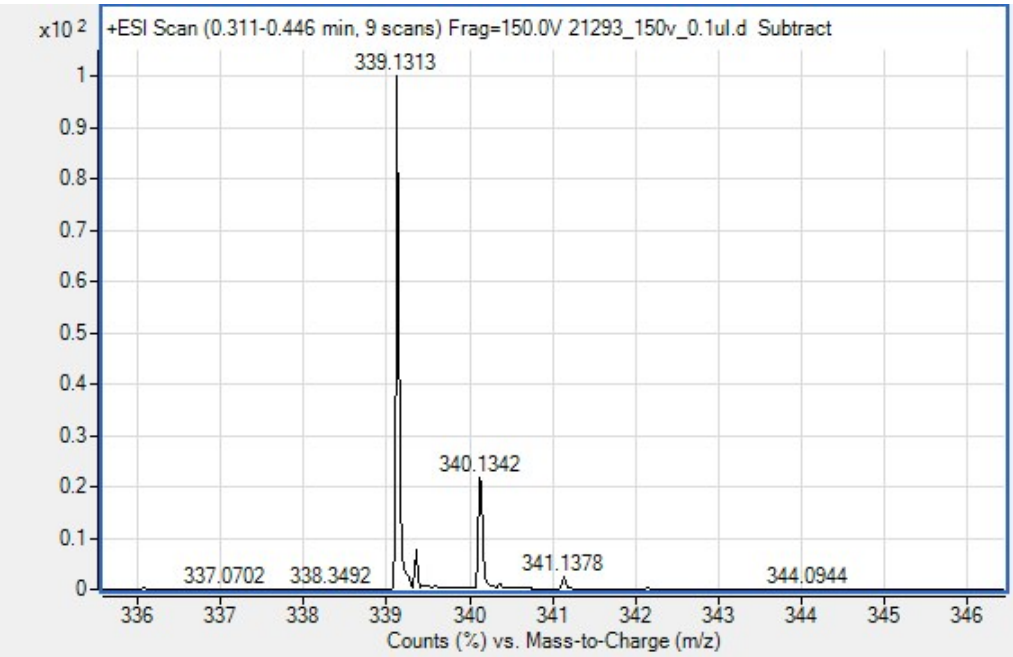

Figure S1-6A Electrospray ionization mass spectrum in positive ion mode for [TPP][TNS]

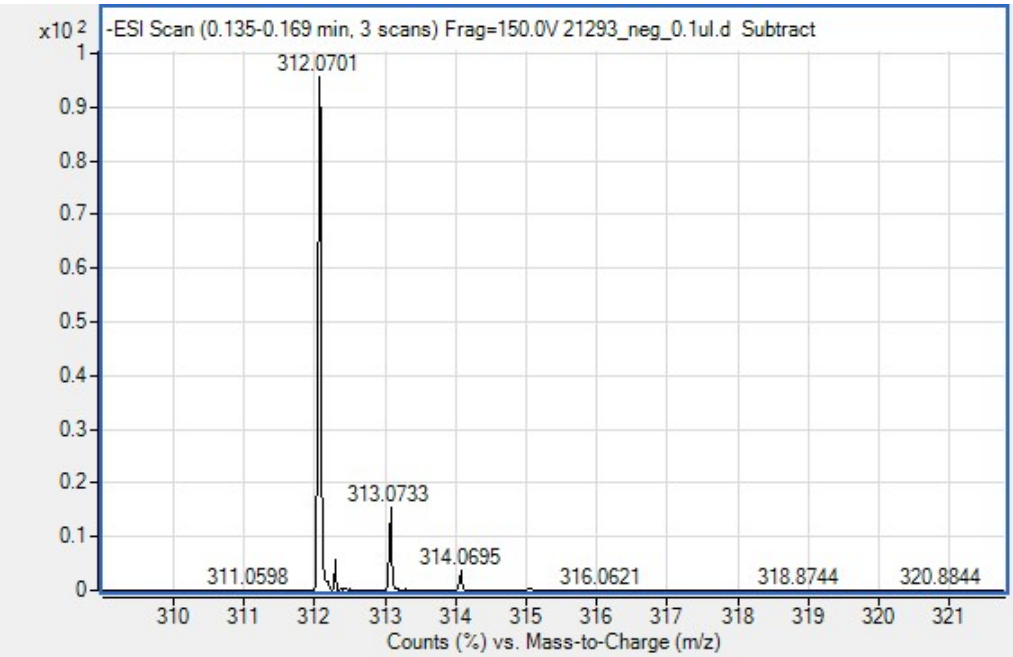

Figure S1-6B Electrospray ionization mass spectrum in negative ion mode for [TPP][TNS]

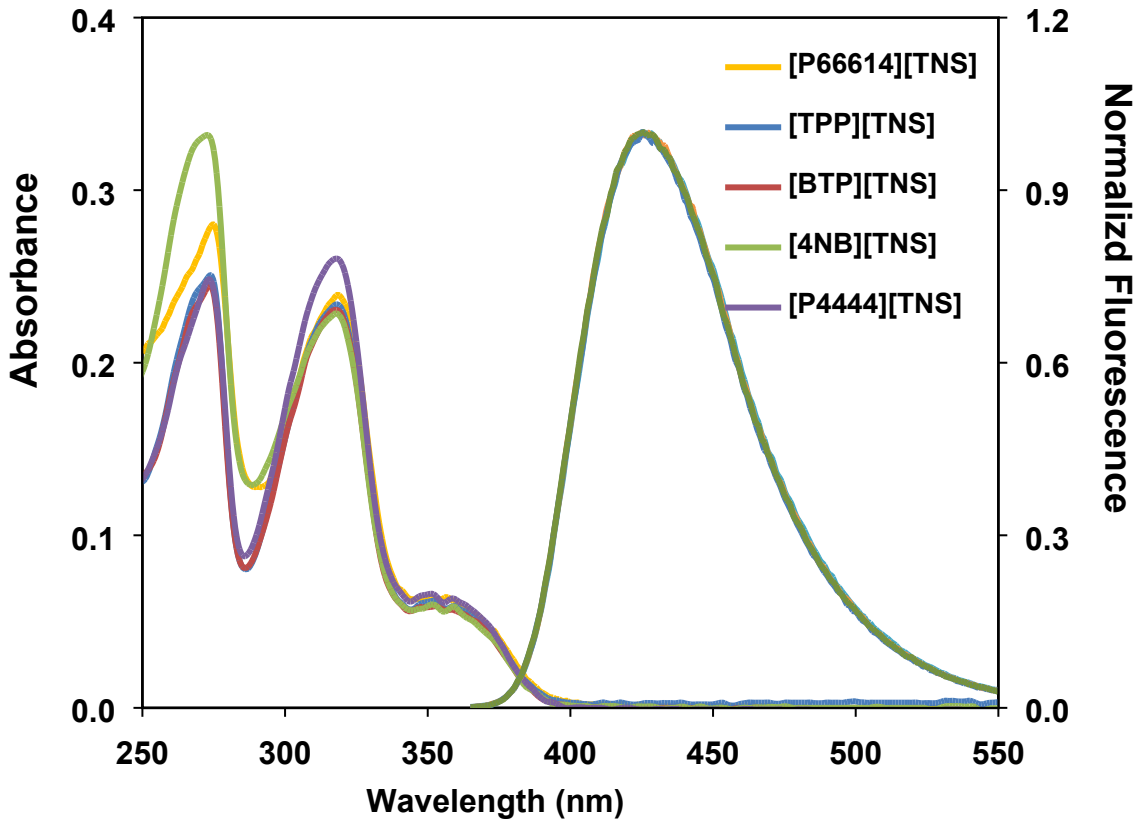

Figure S2. Absorption and fluorescence emission spectra (λ_{ex}- 355 nm) of 10 μM TNS GUMBOS in ethanol. Emission spectrum has been normalized to 1.0 at its maximum.

Table S1. Crystal Data and Structure Refinement for [TPP][TNS], [BTP][TNS] and [P_{4444}][TNS]

	[TPP][TNS]	[BTP][TNS]	[P_{4444}][TNS]
Empirical formula	$C_{24}H_{20}P.C_{17}H_{14}NO_3S.0.7(H_2O)$	$C_{25}H_{22}P.C_{17}H_{14}NO_3S.CH_2Cl_2$	$C_{16}H_{36}P.C_{17}H_{14}NO_3S$
M_r	664.33	750.67	571.77
Crystal system	Monoclinic	Triclinic	Monoclinic
Space group	$P2_1/c$	$P1$	$P2_1/c$
a (Å)	14.3436 (10) Å	10.0089 (4) Å	10.3977 (4) Å
b (Å)	13.8575 (9) Å	10.4658 (4) Å	18.2132 (7) Å
c (Å)	18.0804 (12) Å	10.8995 (4) Å	17.4211 (6) Å
α (deg)		61.537 (2)°	
β (deg)	112.786 (2)°	78.686 (2)°	102.071 (2) °
γ (deg)		66.103 (2)°	
V (Å^3)	3313.3 (4) Å^3	917.68 (6) Å^3	3226.2 (2) Å^3
T (K)	90 K	90 K	90 K
Z	4	1	4

Table S2. Molecular weight (MW), yield (%), melting point (°C), and log $K_{o/w}$, of TNS-based GUMBOS

GUMBOS	MW	Yields (%)	Melting point (°C)	log $K_{o/w}$
[P_{66614}][TNS]	796.22	98	78	1.41
[4NB][TNS]	710.77	99	152	1.09
[P_{4444}][TNS]	571.79	98	162	1.04
[BTP][TNS]	665.78	98	182	1.15
[TPP][TNS]	651.75	99	223	0.78

Table S3. Selected Bond Distances (Å) and Angles (deg) for [TPP][TNS], [BTP][TNS] and [P_{4444}][TNS]

	[TPP][TNS]	[BTP][TNS]	[P_{4444}][TNS]
		Bond Distances	
S1—C1	1.778 (2)	1.7741 (16)	1.767 (5)
N1—C6	1.397 (3)	1.395 (2)	1.377 (6)
N1—C11	1.406 (3)	1.420 (2)	1.395 (7)
N1—H1N	0.84 (3)	0.89 (3)	0.868 (19)
C1—C10	1.361 (4)	1.373 (2)	1.369 (6)
C1—C2	1.412 (3)	1.421 (2)	1.403 (7)
C2—C3	1.370 (3)	1.376 (2)	1.364 (7)
C3—C4	1.415 (3)	1.423 (2)	1.434 (6)
C4—C5	1.419 (3)	1.419 (2)	1.412 (7)
C4—C9	1.425 (4)	1.427 (2)	1.412 (7)
C5—C6	1.380 (3)	1.382 (2)	1.377 (6)
C6—C7	1.422 (4)	1.432 (2)	1.417 (6)
C7—C8	1.358 (4)	1.367 (2)	1.357 (7)
C8—C9	1.421 (4)	1.425 (2)	1.409 (6)
C9—C10	1.409 (4)	1.413 (2)	1.410 (6)
C11—C12	1.397 (3)	1.392 (3)	1.384 (7)
C11—C16	1.395 (4)	1.399 (3)	1.403 (7)
C12—C13	1.391 (3)	1.398 (3)	1.386 (7)
C13—C14	1.395 (4)	1.388 (3)	1.381 (7)
C14—C15	1.390 (4)	1.396 (3)	1.392 (7)
C14—C17	1.504 (4)	1.511 (3)	1.511 (7)
C15—C16	1.392 (4)	1.395 (3)	1.367 (7)
		Bond Angles	
C6—N1—C11	125.6 (2)	123.35 (14)	128.6 (4)
C6—N1—H1N	113 (2)	115.7 (17)	112 (4)
C11—N1—H1N	112 (2)	110.1 (17)	119 (4)
C10—C1—C2	119.9 (2)	120.38 (14)	119.2 (5)
C10—C1—S1	118.79 (18)	119.69 (12)	122.1 (4)
C2—C1—S1	121.28 (18)	119.93 (12)	118.7 (4)
C3—C4—C5	122.9 (2)	122.09 (14)	121.6 (5)
C5—C6—N1	119.5 (2)	124.85 (15)	124.1 (5)
N1—C6—C7	121.3 (2)	116.30 (14)	116.9 (5)
C10—C9—C8	122.1 (2)	122.10 (14)	122.9 (5)
C16—C11—N1	124.4 (2)	118.42 (16)	119.1 (5)
C12—C11—N1	117.5 (2)	122.47 (16)	123.5 (5)

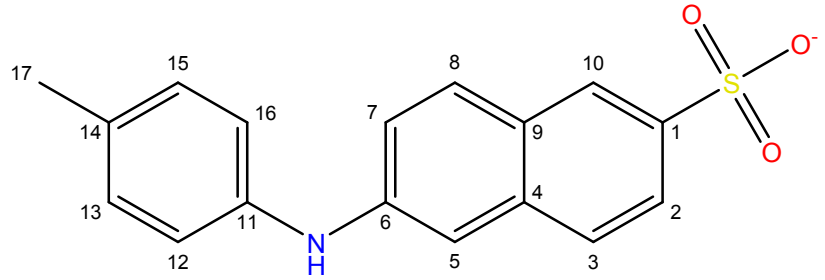

Table S4 Absorption maximum for π – π* transition (λ_{abs}), molar extinction coefficient at 355 nm (ε_{355}), emission maximum (λ_{em}), and quantum yield (φ_{fl}) of TNS-based GUMBOS

GUMBOS	**Solvent**	λ_{abs} **(nm)**	ε_{355}**/10^4 (M^{-1} cm^{-1})**	λ_{em} **(nm)**	% φ_{fl}
[P_{66614}][TNS]	Ethanol	356	6.3	427	5
[4NB][TNS]	Ethanol	352	5.6	425	11
[P_{4444}][TNS]	Ethanol	352	6.1	425	17
[BTP][TNS]	Ethanol	354	5.7	427	11
[TPP][TNS]	Ethanol	353	5.9	425	12

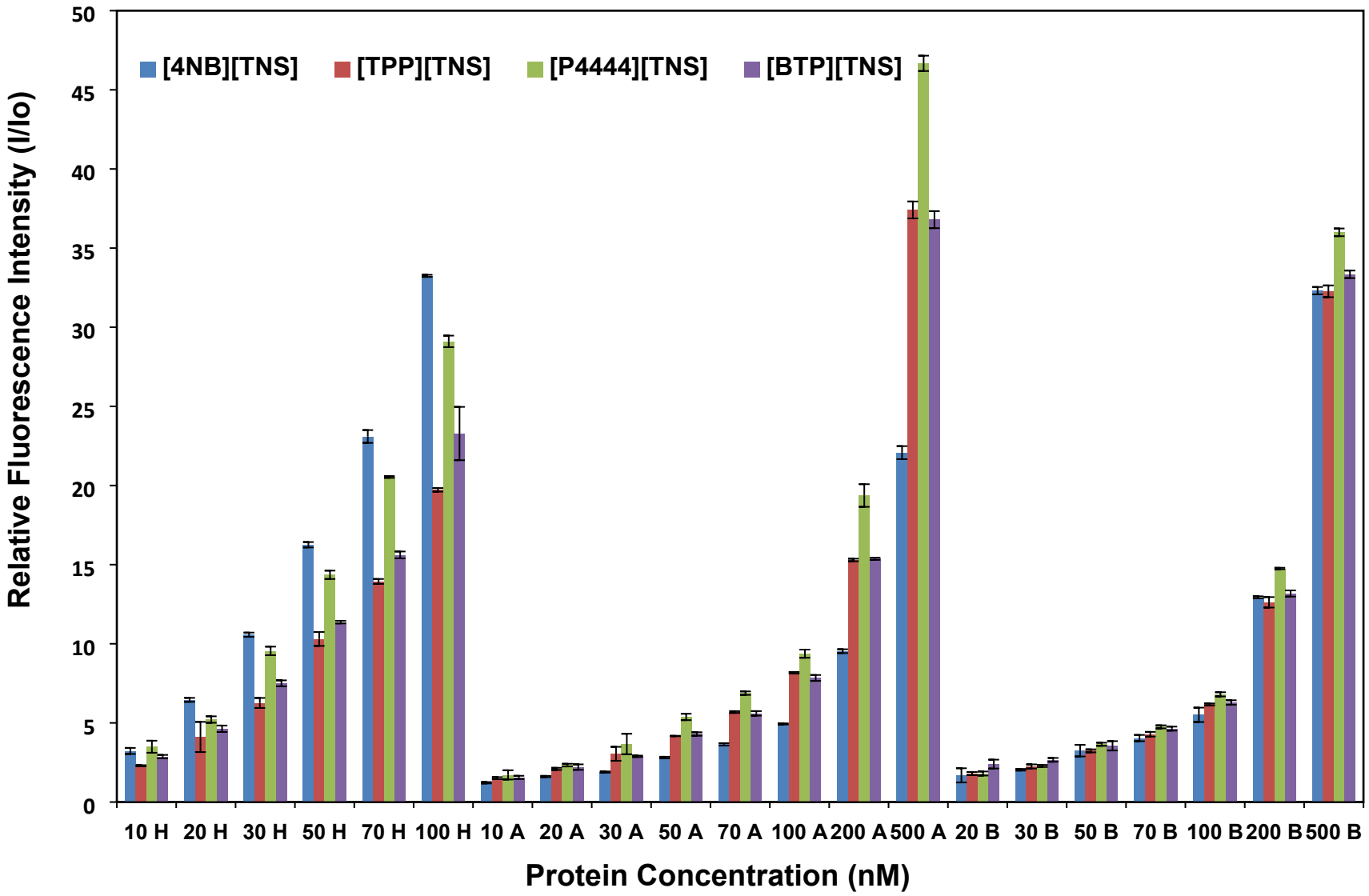

Figure S3 Relative emission intensity (λ_{ex} – 355 nm) of TNS-based GUMBOS at 435 nm in presence of different concentrations of HSA (H), α-antitrypsin (A) and β-lac (B). Error bars represent the standard deviations of five replicate samples

A

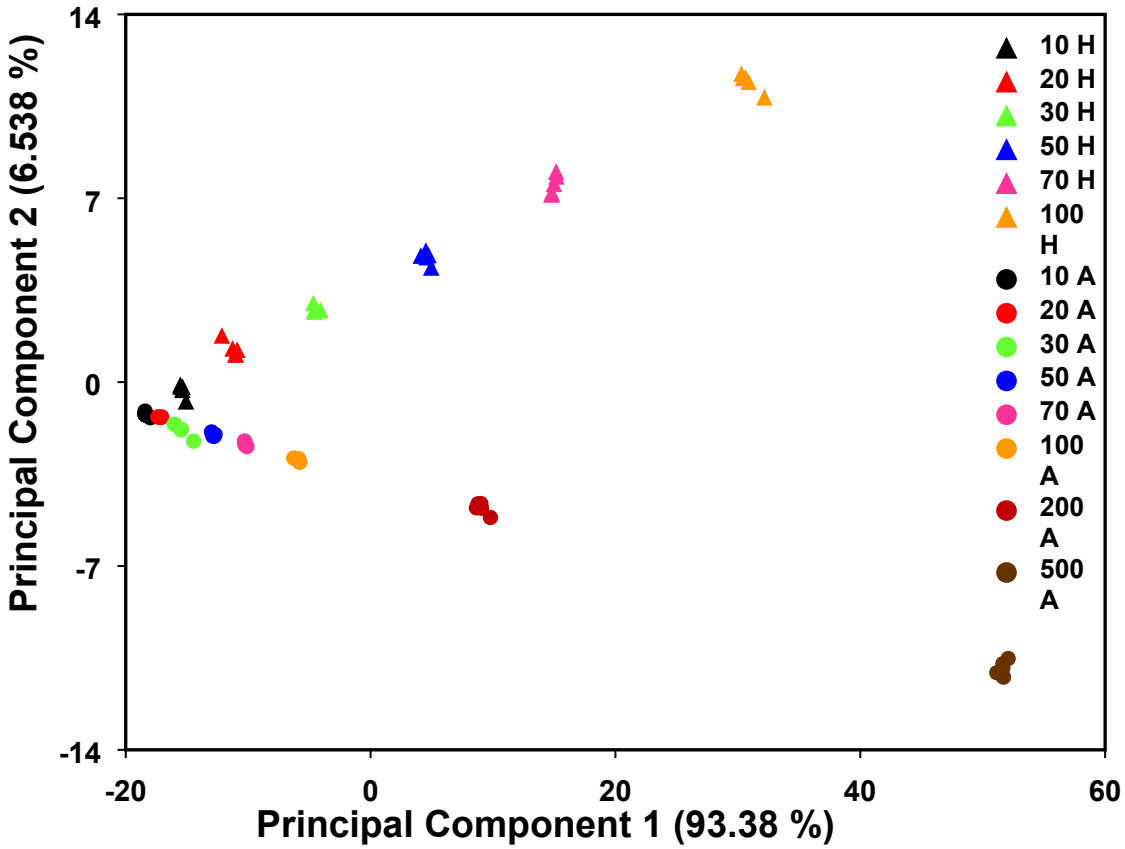
14
7
0
-7
-14
-20
0
20
40
60
Principal Component 2 (6.538 %)
Principal Component 1 (93.38 %)
10 H
20 H
30 H
50 H
70 H
100 H
10 A
20 A
30 A
50 A
70 A
100 A
200 A
500 A

B

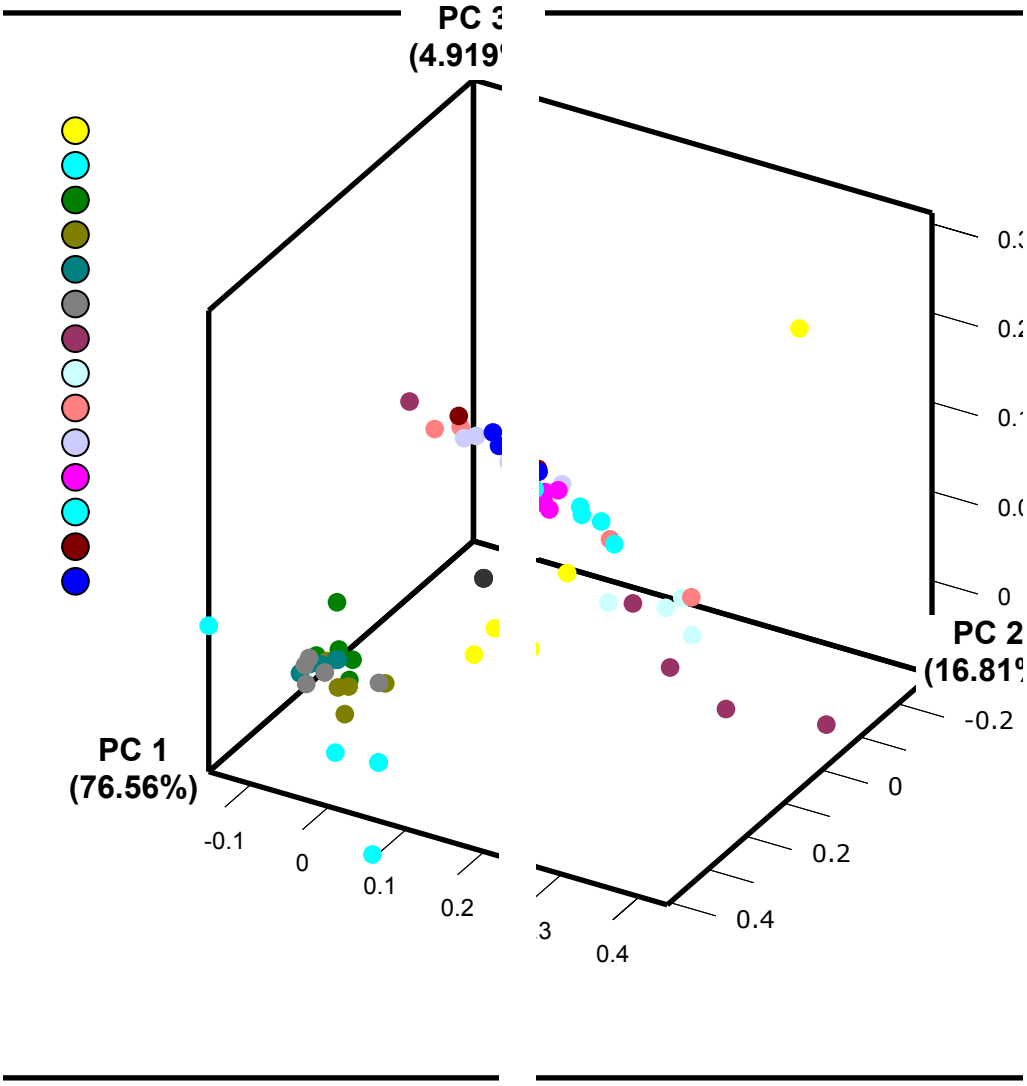

C

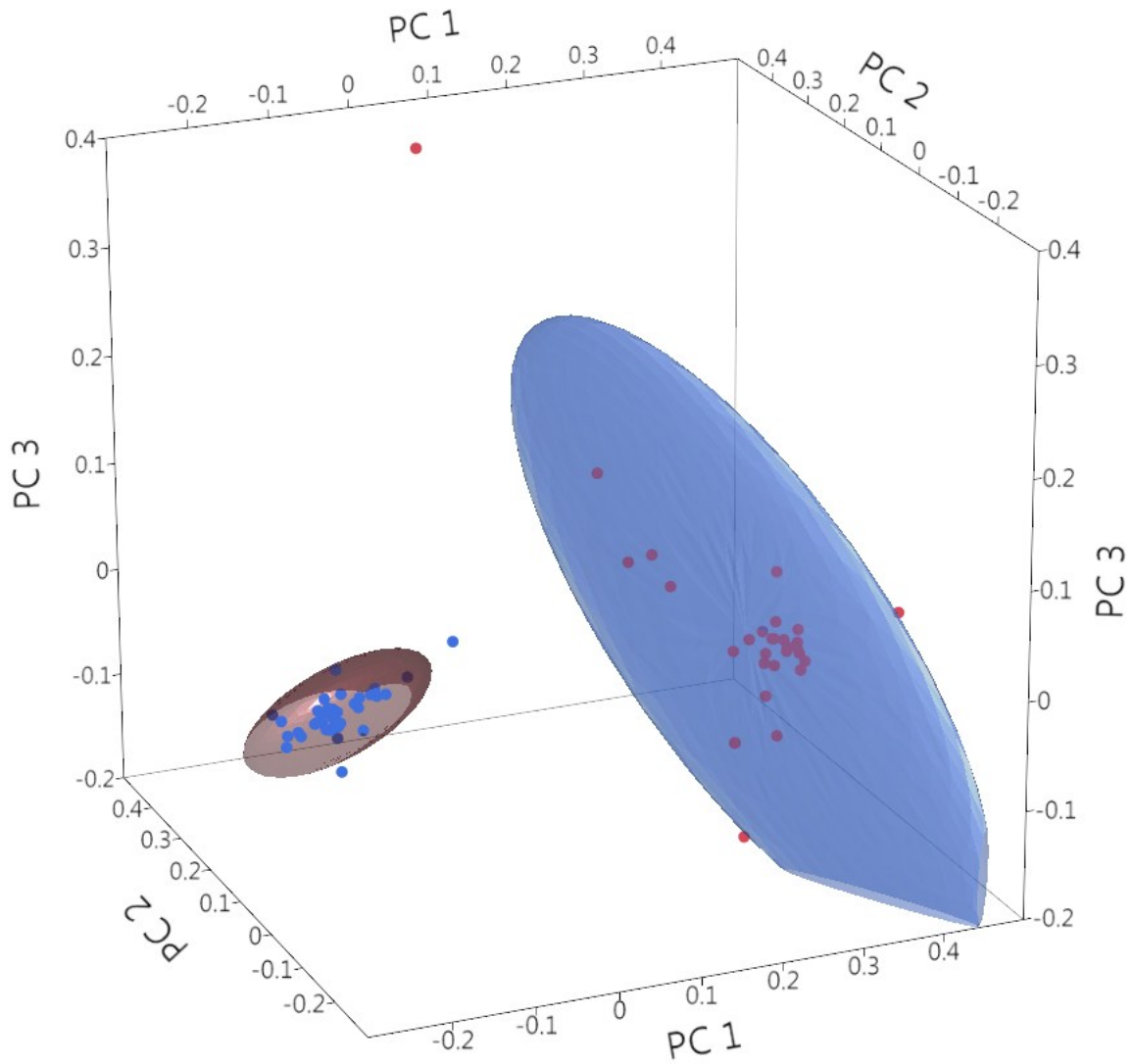

Figure S4. (A) PCA score plot using the first two principal components based on the sensor-response patterns obtained from TNS-based sensors. HSA and α-antitrypsin were labeled as given in the legend (B) PCA score plot using three principal components based on the normalized sensor-response patterns obtained from TNS-based sensors. Different proteins concentrations are given in the legend from top to bottom are 10 nM HSA, 20 nM HSA, 30 nM HSA, 50 nM HSA, 70 nM HSA, 100 nM HSA, 10 Antitrypsin, 20 Antitrypsin, 30 Antitrypsin, 50 Antitrypsin, 70 Antitrypsin, 100 Antitrypsin, 200 Antitrypsin, and 500 Antitrypsin. (C) PCA score plot using three principal components based on the normalized sensor-response patterns obtained from TNS-based sensors: Ellipsoids cover 95% of each cluster; HSA – blue ellipsoid, α-antitrypsin – red ellipsoid

A

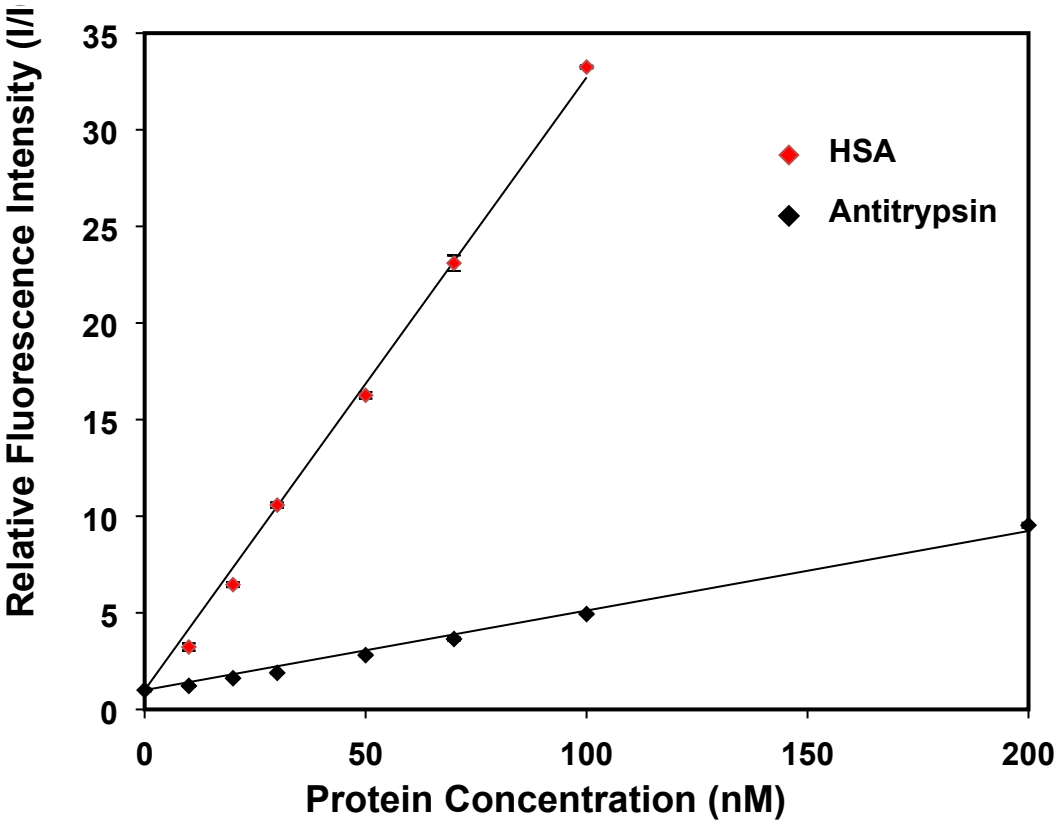
Relative Fluorescence Intensity (I/I
35
30
25
20
15
10
5
0
0
50
100
150
200
Protein Concentration (nM)
HSA
Antitrypsin

B

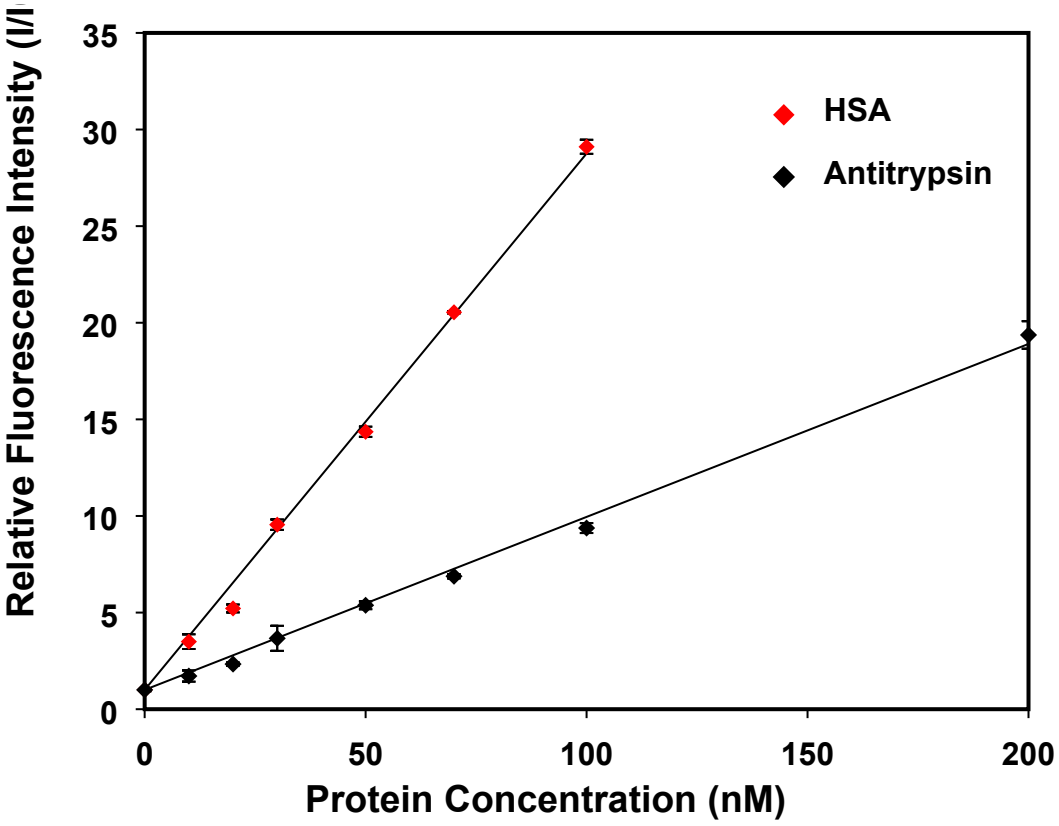
Relative Fluorescence Intensity (I/I
35
30
25
20
15
10
5
0
0
50
100
150
200
Protein Concentration (nM)
HSA
Antitrypsin

C

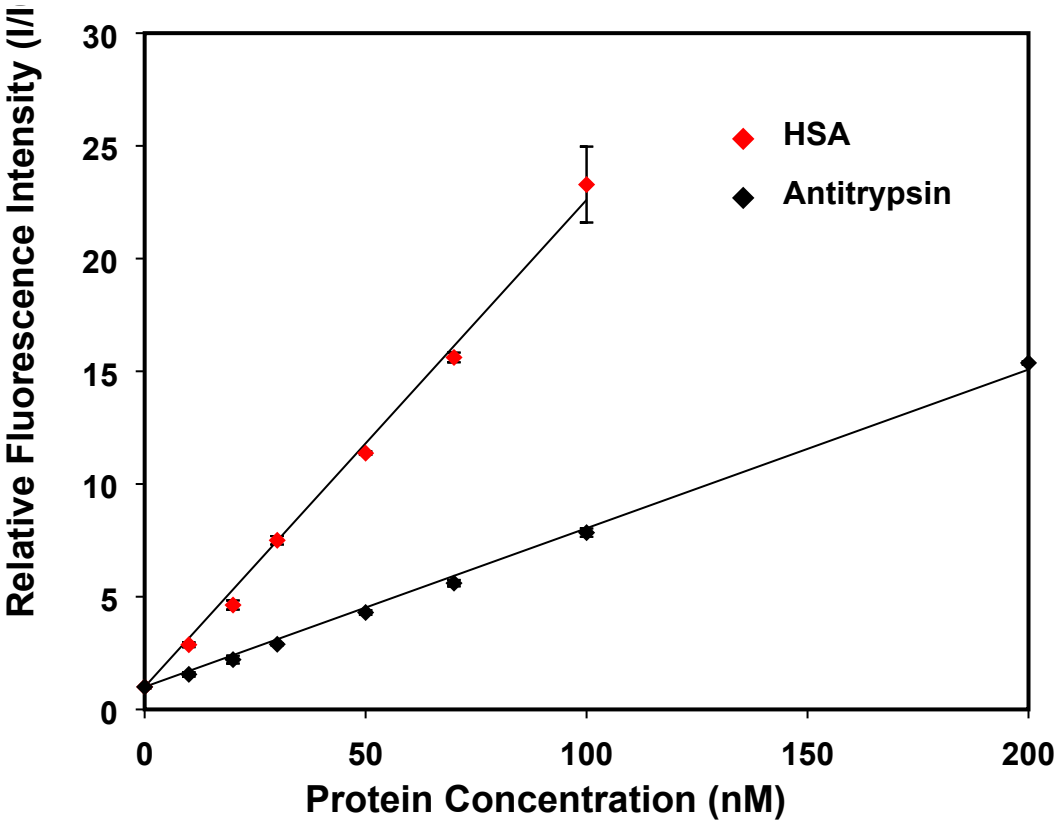
Relative Fluorescence Intensity (I/I
30
25
20
15
10
5
0
0
50
100
150
200
Protein Concentration (nM)
HSA
Antitrypsin

D

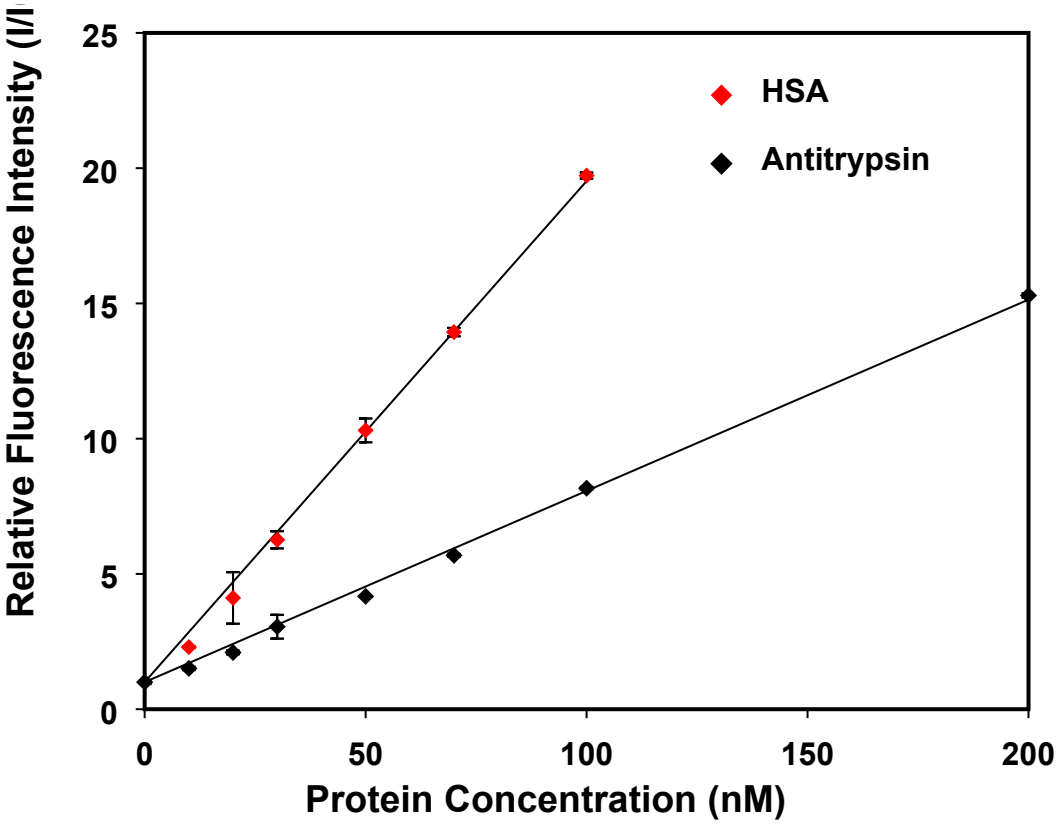
Relative Fluorescence Intensity (I/I
25
20
15
10
5
0
0
50
100
150
200
Protein Concentration (nM)
HSA
Antitrypsin

Figure S5. Plot of relative fluorescence emission intensity *versus* the concentration of HSA (red), or α-antitrypsin (black) for (A) [4NB][TNS], (B) [P_{4444}][TNS], (C) [BTP][TNS], and (D) [TPP][TNS]. Error bars represent the standard deviations of five replicate measurements

(1) Sheldrick, G. M.: A short history of SHELX. *Acta Crystallographica Section A: Foundations of Crystallography* **2007**, *64*, 112-122.

(2) Spek, A. L.: Structure validation in chemical crystallography. *Acta Crystallographica Section D: Biological Crystallography* **2009**, *65*, 148-155.

(3) Das, S.; de Rooy, S. L.; Jordan, A. N.; Chandler, L.; Negulescu, I. I.; El-Zahab, B.; Warner, I. M.: Tunable Size and Spectral Properties of Fluorescent NanoGUMBOS in Modified Sodium Deoxycholate Hydrogels. *Langmuir* **2012**, *28*, 757-765.